Development of a non-destructive stress measurement method using distributed fiber optic sensing and geophysical techniques

Sepidehalsadat Hendi
Geological Engineering/Earth, Ocean and Atmospheric Sciences, The University of British Columbia, Vancouver, Canada

Erik Eberhardt
Geological Engineering/Earth, Ocean and Atmospheric Sciences, The University of British Columbia, Vancouver, Canada

Mostafa Gorjian
Geological Engineering/Earth, Ocean and Atmospheric Sciences, The University of British Columbia, Vancouver, Canada

ABSTRACT: In-situ stress is a critical boundary condition that dictates many important rock engineering design decisions such as the orientation, dimensioning and support design of underground excavations for mining and civil infrastructure to ensure stability and safety, as well as the optimal orientation of horizontal boreholes for energy development projects (geothermal, unconventional gas). However, it is also one of the most difficult parameters to measure reliably, resulting in significant uncertainty and risk to these projects. This has seen the development of numerous stress measurement techniques, each with its limitations and reliability issues. Presented here are the first steps in the conceptualization and workflow for a non-destructive stress measurement technique using distributed fiber optic sensing and geophysical techniques that overcomes several key challenges and limitations, while adding value through increased measurement resolution and reliability. Numerical workflow results are presented that compare favorably with values based on experimental results.

Keywords: In-situ stress, distributed sensing, fiber optics, stress measurement, borehole geophysics.

1 INTRODUCTION

Engineering analyses require boundary conditions. One of the most important of these for rock engineering design is the in-situ stress state. The in-situ stress is a tensor quantity, and it dictates many of the most important design decisions regarding excavation stability, orientation optimization and support design to ensure safety, as well as borehole stability and induced fracture orientation in the case of hydraulic fracturing for geothermal and unconventional gas development. However, it is also one of the most difficult parameters to measure, and to do so reliably and with confidence. It is not uncommon for stress measurements to indicate two conflicting stress regimes, resulting in significant uncertainty and risk to these projects. This frequently leads to less-than-optimal design performance and costly mistakes. Numerous stress measurement techniques exist, each with significant limitations and reliability issues. These are generally divided into two approaches (Amadei & Stephansson, 1997). The first involves measuring strain responses, for example, the strain relief from overcoring, from which the in-situ stress field is inverted (Sjöberg et al., 2003). These

suffer from reliability issues related to conformability where it is necessary to ensure that the measurement probe is properly attached to the rock. More importantly, they are limited to point measurements. A rock mass is rarely homogeneous and isotropic, and thus because these point measurements are made in boreholes, they are blind to any heterogeneity that may be present in the larger rock volume that can affect the measured strain response. The second approach is to measure the pressure required to hold a fracture of a given orientation open, for example, that generated through hydraulic fracturing, which gives stress information for that direction (Haimson & Cornet, 2003). Although these involve larger rock volumes, they suffer from being destructive, generating new fractures in the rock that limit repeat validation testing and can later affect the strength and permeability of the rock (where these might be prohibitive, for example in the case of a nuclear waste repository). In addition to being destructive, these methods are only able to measure the stress through considerable effort that often restricts them to being made at a single point in time (where repeat measurements of stress change over time might be desired).

Ideally, the use of a non-destructive technique that can measure both the in-situ stress state but also any subsequent stress changes in response to engineering activities (e.g., mining) would be advantageous. Even more so if the technique can do so for a larger representative volume of rock, measuring the far-field state away from a borehole, as well as along the length of a borehole to sample multiple locations relative to changes in the geology. A common non-destructive measurement technique is based on acoustic/seismic velocities (P- and S-wave) and distributed sensing. Acoustic velocity represents a high-resolution measurement that is sensitive to stress, that is transmitted into the rock mass, and can be carried out from a fixed measurement device for longer monitoring periods.

This paper presents the initial results towards the testing of a new non-destructive stress measurement technique we are developing based on distributed sensing and fiber optics. Our research indicates that distributed fiber optic sensing has promising potential to overcome existing stress measurement challenges while also adding value through improved measurement resolution, repeatability and reliability. The results presented focus on a 3-D numerical workflow to support lab-scale testing, generated to simulate seismic wave propagation within an instrumented rock sample subjected to hydrostatic loading with the capability to consider real-field conditions like rock anisotropy.

2 BACKGROUND

A significant amount of laboratory testing research has been conducted to investigate the effects of confining pressure on both the dynamic and static elastic constants of rock. The results of these studies have shown that seismic velocities in rocks are generally sensitive to stress, increasing with increasing stress. This is generally attributed to the closing of compliant, crack-like pore space, including microcracks and grain boundaries. As confining pressure is raised, the most compliant cracks/pores are closed, followed by the next most compliant, and so on. Closing pores increase the mechanical stiffness of the rock, and in turn, its acoustic velocities (Mavko & Godfrey, 1995; Wang, 2002; Sone & Zoback, 2013; Melendez, 2014; Hawkes et al. 2015). The same observation is made regarding the static stiffness characteristics of rocks.

Rocks can also be anisotropic. This generally results from a layering of mineral grains, fractures, and/or differential stresses in bedded rock masses. In anisotropic medium, seismic waves propagate in different directions with different velocities. Based on this fact, it would be expected that after triggering a seismic source in an anisotropic formation, shear waves will propagate faster in the direction of the maximum in-situ stress and slower in the direction of the minimum in-situ stress. Using measured shear wave velocities, the elastic stiffness constants can be determined. By replacing the field-calculated elastic stiffness constants with experimental relations between stress and elastic stiffness, the in-situ stresses can be determined. Furthermore, the fastest shear velocity is in the direction of the maximum stress, allowing the orientation of the in-situ stress to be determined as well. The following relationship exists between applied stress and strain in elastic materials:

$$\sigma_{ij} = C_{ijkl}\varepsilon_{kl} \quad (1)$$

where C_{ij} , σ_{ij}, and ε_{kl} represent the elastic stiffness constants, stresses, and strains, respectively. Building on this, Table 1 presents several equations that relate phase velocities to dynamic elastic constants in a medium with transverse isotropic symmetry (TI). This serves as a reasonable approximation for rock anisotropy where the medium has an axis of rotational symmetry in which 5 elastic constants are required to fully describe it.

Table 1. Elastic stiffness constants, C_{ij}, for a transverse isotropic medium, where ρ is the material density and V_p and V_s are the compressional- and shear-wave velocities, respectively.

Dynamic Elastic Stiffness	Polarization Direction
$C_{11} = \rho V_P^2$	(Along any n within the xy-plane)
$C_{22} = \rho V_P^2$	(Same as C_{11})
$C_{33} = \rho V_P^2$	(Along n=$[0, 0, \pm 1]$)
$C_{44} = \rho V_S^2$	(With polarization $[0, 0, \pm 1]$ along any n within the xy plane)
$C_{44} = C_{55}$	
$C_{66} = \rho V_S^2$	(With polarization $[0, \pm 1, 0]$ along n = $[\pm 1, 0, 0]$ or with polarization $[\pm 1, 0, 0]$ along n= $[0, \pm 1, 0]$)
$C_{13} = C_{11} - 2C_{66}$	
$C_{12} = \rho V_P^2 - 2C_{44} - C_{11}$	(Along n=$\left[0, \pm \frac{1}{\sqrt{2}}, \pm \frac{1}{\sqrt{2}}\right]$ or $\left[\pm \frac{1}{\sqrt{2}}, 0, \pm \frac{1}{\sqrt{2}}\right]$)

3 METHODOLOGY

A key first step in developing our in-situ stress measurement technique was to conduct laboratory-scale, proof-of-concept testing. The tests integrate a fiber optic sensor and interrogator with a high capacity triaxial loading system. To support these tests, it was necessary to generate a numerical workflow and model, which could be used to determine the stress dependence of each of the dynamic elastic stiffness moduli comprising the transversely isotropic stiffness tensor for an instrumented rock sample. Here, it was assumed that the applied stresses and elastic stiffness constants followed a linear relationship under hydrostatic loading, given by:

$$C_{ij} = a_{1_{ij}} (\sigma_1 + \sigma_2 + \sigma_3) + a_{2_{ij}} \quad (2)$$

where $a_{1_{ij}}$ and $a_{2_{ij}}$ represent the slope and intercept, respectively, of the line fitted to the experimental data.

These relations were used as input for a 3-D numerical model developed in Itasca Consulting Group's FLAC3D^{TM} to simulate seismic wave propagation within a rock sample subjected to hydrostatic loading inside the triaxial cell. It was assumed that seismic waves were recorded by a fiber optic sensor cemented inside a central hole drilled into the rock sample. It was also assumed that the fiber optic sensor was helically wrapped (at a 30-degree angle) to increase its broadside sensitivity. The model geometry and boundary conditions are shown in Figure 1.

In this numerical model, seismic energy was emitted by a point source located on the exterior surface of the rock sample, close to its bottom. To record the response of the fiber optic sensor, a number of virtual points were defined as an array of gauges along the length of the sensor. In order to minimize the reflections from the model boundary, a quiet boundary was used (see Figure 1). The results of the stimulation were then assessed and verified against results generated using an analytical solution.

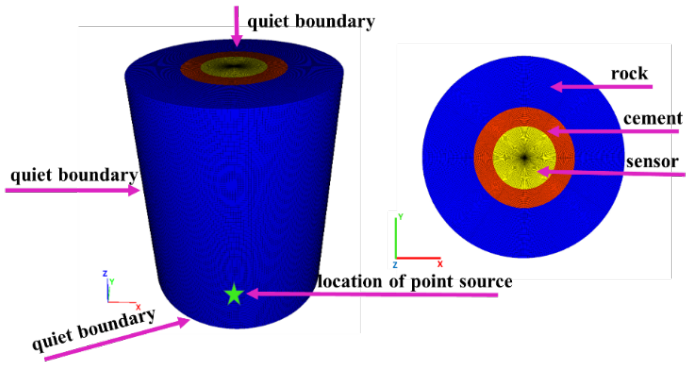

Figure 1. FLAC3DTM model geometry to simulate fiber-optic stress measurement testing condition. The different domains are identified by the different colors. The model is surrounded by quiet boundary conditions. The location of the seismic point source is shown with a star.

4 RESULTS

Dynamic elastic stiffness constants (C_{ij}) were calculated based on measured velocities under hydrostatic loading. Each elastic constant was plotted against the mean stress and a trendline fitted through the data points. Table 2 lists the linear trendline parameters for each elastic constant.

Figures 2 shows an example from the numerical modeling results simulating the response of the fiber optic sensor under hydrostatic loading. Figure 2a shows the generation of the waveforms from the point source towards the sensor located at the center of the rock sample. Figure 2b illustrates the modeled waveforms recorded by the sensor. The shear wave velocity calculated from the stimulation closely matches the experimental results. The seismic energy reached the sensor at approximately 2 milliseconds, as seen in the recorded waveforms. When this wave reaches the other side of the cable-cement interface, some energy is reflected back in the sensor as a result of the contrast in material properties between the two domains.

Table 2. Input parameters used for the numerical analysis and verification exercise.

Dynamic Elastic Stiffness Constants of Rock Sample					
		a_1(-)		a_2(GPa)	
C_{11}		64.30		58.75	
C_{33}		245.43		32.48	
$C_{44}(=C_{55})$		228.55		19.84	
C_{66}		16.41		22.76	
$C_{12}(=C_{21})$		28.22		13.33	
$C_{13}(=C_{23})$		108.86		9.70	
Static Elastic Properties					
ρ (kg/m^3)	G_v(GPa)	$E_v(GPa)$	$E_h(GPa)$	$\vartheta_v(-)$	$\vartheta_h(-)$
2600	7.1	15.4	31.2	0.2	0.08
Cement Properties					
Density (kg/m^3)		Shear Modulus (GPa)		Bulk Modulus (GPa)	
2240		6.3		8.3	
Cable Properties					
Density (kg/m^3)		Shear Modulus (GPa)		Bulk Modulus (GPa)	
1200		0.7		0.8	
Hydrostatic Loading (MPa)		Seismic Source			
		Dominant Frequency (Hz)		Amplitude (MPa/s)	
30		8000		5	
Geometry					

Rock		Cement		Cable	
Height(mm)	Diameter(mm)	Height(mm)	Diameter(mm)	Height(mm)	Diameter(mm)
152	76	152	50	152	25

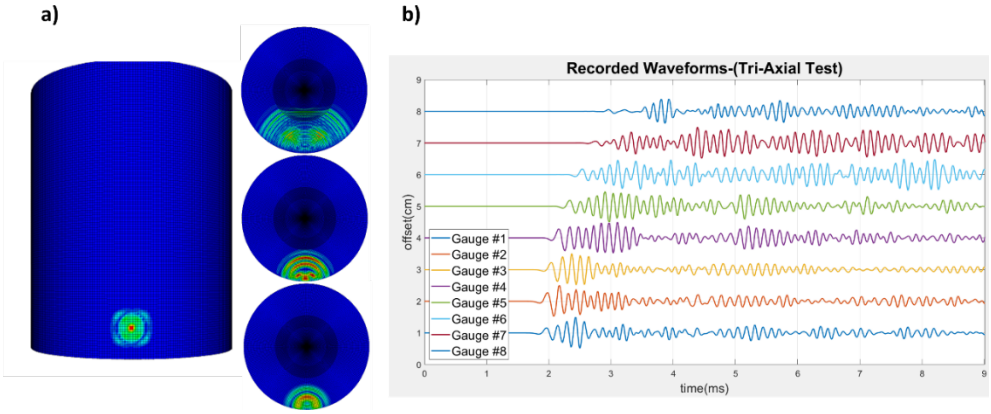

Figure 2. a) Propagation of the simulated seismic wave, from its point source to the fiber optic sensor as a function of different time steps. b) The waveforms recorded by the sensor in the middle of the rock sample.

5 FUTURE WORK

The next steps in our work will make use of the verified numerical model to optimize the work flow and validate it against field measured data. This motivates an inverse problem written as:

$$FS_i\,[m] + N_i = OD_i \tag{3}$$

where *FS* is the forward simulation operator (i.e., the numerical simulation incorporating relevant physical properties, physical equations and sources properties), *m* is a generic symbol for the inversion model, *N* is the noise, which is often assumed to have known statistics, and *OD* is the observed data. The goal is to recover the magnitude of the in-situ stresses, *m*. Finding a model based solely on data is an ill-posed problem because there is no unique solution. Additional information must be included based on prior knowledge and assumptions, for example those related to temperature, the seismic source property and anisotropy orientation. These are then updated/modified during the inversion to obtain optimal responses. Defining and solving a well-posed inverse problem is a complex task that requires many components that must interact. Viewing this task as a workflow in which various elements are explicitly identified and integrated is advantageous. Figure 3 shows the inversion methodology, which includes inputs, implementation, and evaluation.

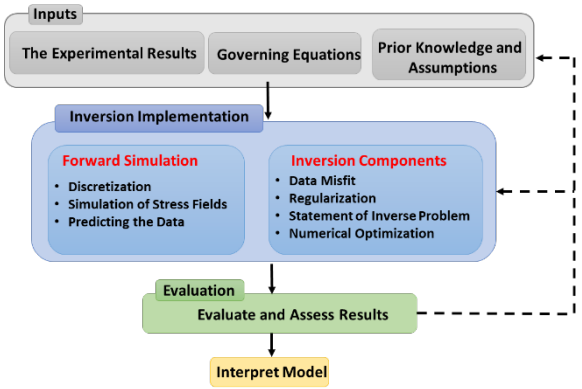

Figure 3. Workflow of inversion for estimating in-situ stress from measured shear wave velocities.

6 CONCLUSIONS

A numerical modeling workflow was developed to enable the calculation of the response of a fiber optic sensor cemented within a rock sample to a seismic source under different loading conditions. The results of the simulation compare favorably with estimated values based on analytical solutions and experimental results. As such, it was concluded that the workflow is effective and appropriate to serve as a means to advance inversions to derive in-situ stress information from distributed fiber optic field-scale sensing measurements and data. The inversion method will be used to optimize the workflow by comparing the seismic stimulation results against the field data and updating the assumptions and unknowns.

The validated workflow will aid in the advancement of a novel stress measurement technique which differs from available techniques as follows: i) provides both the stress magnitudes and orientations in one measurement (some techniques require multiple measurements); ii) non-destructive measurement technique (i.e., measurement can be repeated for added precision and confidence); iii) measures stress state for a large volume of rock (i.e., is less susceptible to misleading measurements due to rock mass heterogeneity); and iv) can be used to measure a stress profile along a borehole, and through repeat surveys, stress changes over time.

ACKNOWLEDGEMENTS

The authors would like to thank Innovate BC and their Ignite program, the Centre for Innovation in Mineral Resource Engineering (CIMRE), Geoscience BC and the Natural Sciences and Engineering Research Council of Canada (NSERC) for their financial support.

REFERENCES

Amadei, B. & Stephansson, O. 1997. *Rock stress and its measurement*. Chapman & Hall: London.

Haimson, B.C. & Cornet, F.H. 2003. ISRM suggested methods for rock stress estimation—Part 3: hydraulic fracturing (HF) and/or hydraulic testing of pre-existing fractures (HTPF). *International Journal of Rock Mechanics and Mining Science* 40, pp. 1011–1020.

Hawkes, R.V., Anderson, I., Bachman, R.C. & Settari, A. 2013. Interpretation of closure pressure in the unconventional Montney using PTA techniques. In: *SPE 2013 Hydraulic Fracturing Technology Conference*, The Woodlands, Texas, pp. 4-6.

Ljunggren, C. 1999. *Rock stress measurements by means of hydraulic methods at Hästholmen, 1998–1999*. Working Report 99-54, Posiva Oy, Finland.

Mavko, G., Mukerji, T. & Godfrey, N. 1995. Predicting stress-induced velocity anisotropy in rocks. *Geophysics* 60(4), pp. 1081-1087.

Melendez Martinez, J. 2014. *Elastic properties of sedimentary rocks*. Ph.D. thesis, University of Alberta, Canada.

Sjöberg, J., Christiansson, R. & Hudson, J.A. 2003. ISRM suggested methods for rock stress estimation—Part 2: overcoring methods. *International Journal of Rock Mechanics and Mining Science* 40, pp. 999–1010.

Sone, H. & Zoback, M.D. 2013. Mechanical properties of shale-gas reservoir rocks- Part 1: static and dynamic elastic properties and anisotropy. *Geophysics* 78(5), pp. D381-D392.

Wang, Z. 2002. Seismic anisotropy in sedimentary rocks, Part 2: laboratory data. *Geophysics* 67(5), pp. 1423-1440.